NASA CR-112117

DEVELOPMENT AND EVALUATION OF A DEVICE TO SIMULATE A SONIC BOOM

by

L. C. Rash, R. F. Barrett, and F. D. Hart

Center for Acoustical Studies
Box 5801
North Carolina State University
Raleigh, North Carolina 27607

REPORT PREPARED UNDER

NASA RESEARCH GRANT NGL 34-002-095

May 1972

SUMMARY

A device to simulate the vibrational and acoustical properties of a sonic boom was developed and evaluated. The design employed a moving circular diaphragm which produced pressure variations by altering the volume of an air-tight enclosure that was located adjacent to an acoustical test chamber. A review of construction oriented problems, along with their solutions, is presented. The simulator is shown to produce the effects of sonic booms having pressure signatures with rise times as low as 5 milliseconds, durations as short as 80 milliseconds, and overpressures as high as 2.5 pounds per square foot. Variations in the signatures are possible by independent adjustments of the simulator. The energy spectral density is also shown to be in agreement with theory and with actual measurements for aircraft.

TABLE OF CONTENTS

LIST OF FIGURES

LIST OF FIGURES (continued)

INTRODUCTION

Whenever an object travels through the atmosphere at velocities greater than the speed of sound, a pressure wave is generated that emanates from the object and produces an explosive sensation in the auditory system of humans and animals. When the above phenomena is associated with aircraft, it is generally referred to as a sonic boom. This occurrence can have an annoying or even startling effect on the populace, but restricting it to a particular location and a convenient time would be difficult. An alternative is to determine the physiological effect of the noise and vibration caused by the sonic booms on man. To perform such a study requires a device that can adequately simulate both the acoustical and the vibrational properties of a sonic boom. The purpose of this research was to produce such a sonic boom simulator, which would later be applied to a study of the effects of sonic booms on peoples' sleep patterns.

REVIEW OF LITERATURE

There are generally three basic approaches used for controllable sonic boom simulators within a laboratory. They are the headset method, the progressive wave method, and the chamber vibration method. The headset method used electronic speakers mounted inside an acoustical chamber to produce realistic indoor acoustic simulation but lacked vibration stimulus. The progressive wave method produces ground shock waves by an explosive source and a magnifying expansion tube but also does not create the vibrations associated with sonic booms. The chamber vibration method gives the best indoor acoustical and vibrational simulation by changing the volume of an airtight chamber with a machine that moves a portion of the chamber wall. The final method was used in a design that was proposed by Redman (8) and supported by the National Aeronautics and Space Administration. This design included the following general steps of a design process:

a. problem definition
b. feasibility study
c. preliminary design
d. detail design.

The remaining steps that would complete the design process are listed below:

e. construction
f. development
g. testing
h. evaluation.

Items e, f, g, and h provide a physical application and analysis of the principles developed earlier in the design process.

DEVELOPMENT AND CONSTRUCTION

Test Chamber

After the initial design, it became apparent that additional testing facilities would be required. The laboratory that was originally intended to be used presented a space limitation. Also, additional studies with acoustic stimuli had been initiated, so inevitably, a new test chamber was designed and built for use on the sleep study project.

The dimensions of the test chamber were determined by the size of the laboratory, the equipment arrangement, and an allowance for access around the equipment. The arrangement in the laboratory is shown in Figure 1. Standard house construction procedures were used in the design of the test chamber so that the vibrational characteristics would be similar to those produced by an actual sonic boom. Figures 2 and 3 indicate the construction techniques employed and the dimensions. Basically, plywood covered the floor joists and the exterior side of the wall studs and sheet rock was used for the interior walls and ceiling. The walls were fitted with wall receptacles, a ventilation fan, and an interior type door with frame. A support for the ventilation fan was mounted on the plywood wall surface but secured to the stud wall. After the walls had been finished and painted, an overhead light and carpeting were installed. A bed, dresser, and chairs gave the test chamber the desired appearance of a bedroom.

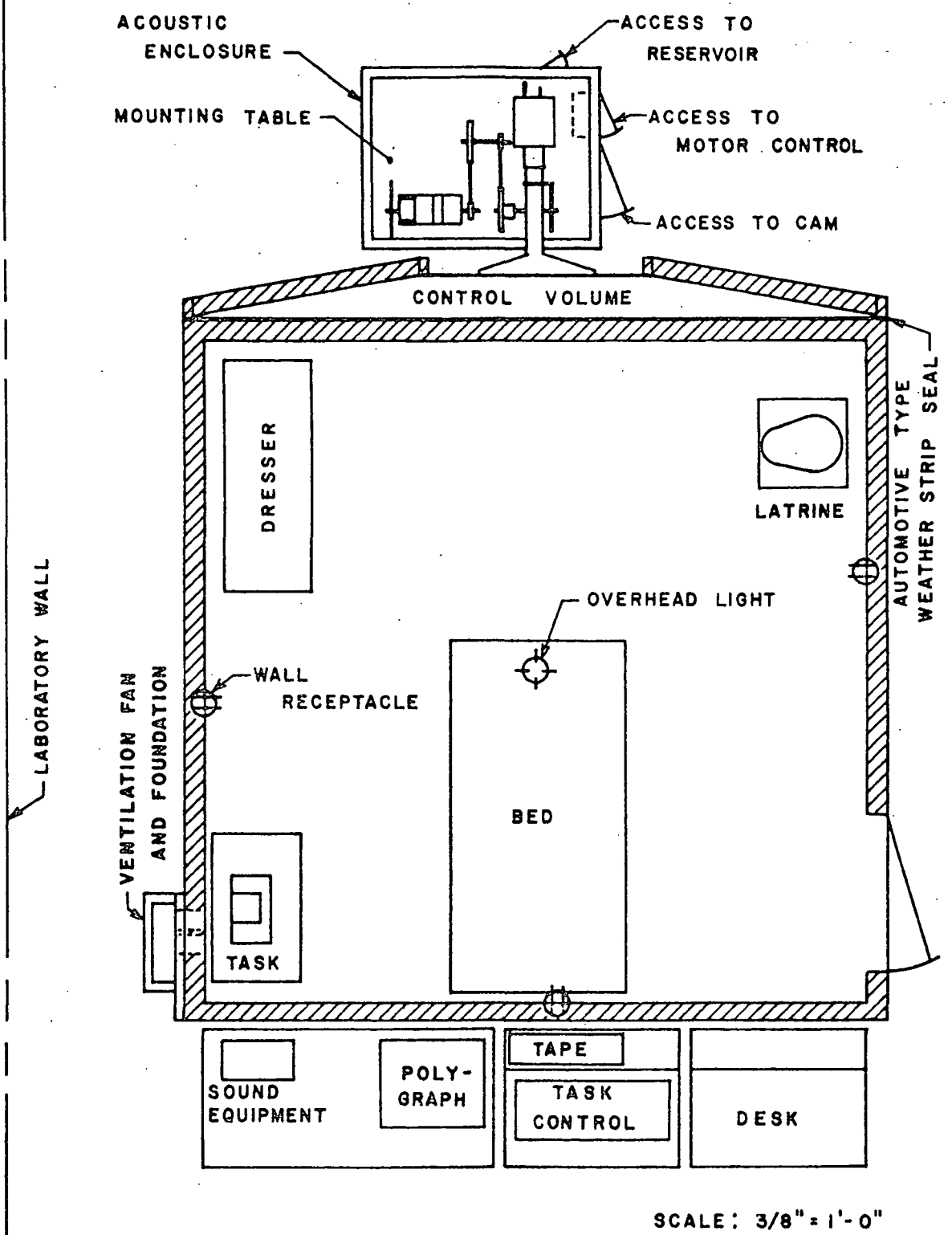

Figure 1. Laboratory equipment arrangement

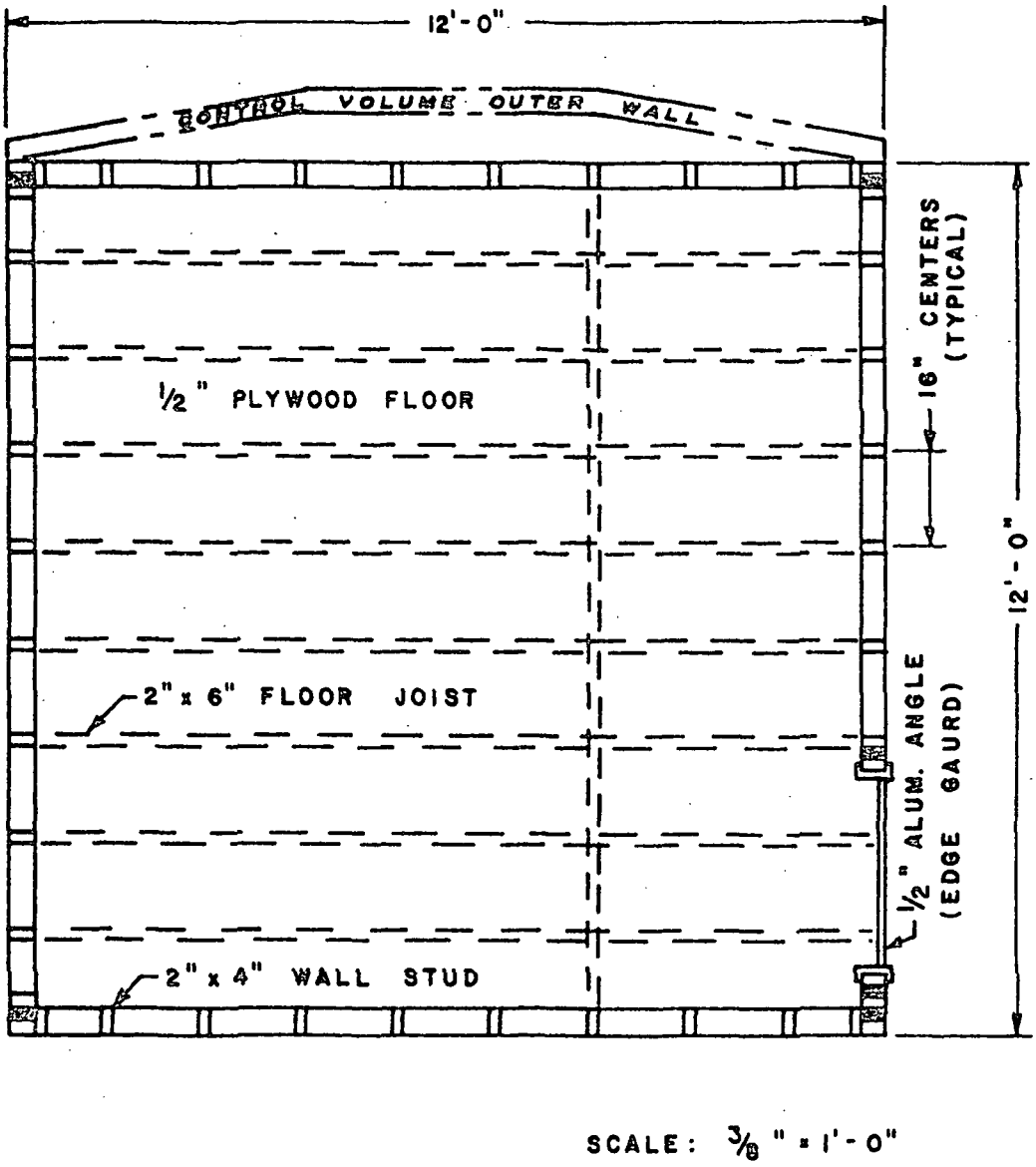

Figure 2. Test chamber floor plan

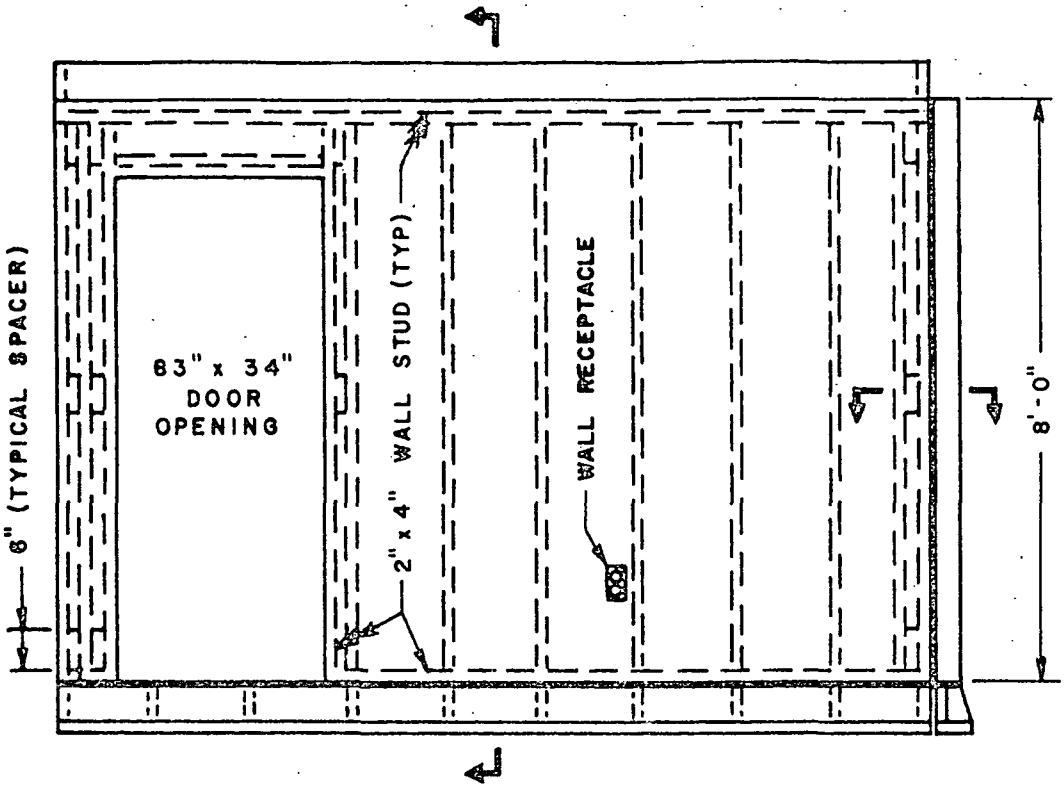

FRONT WALL SCALE: 3/8" = 1'-0"

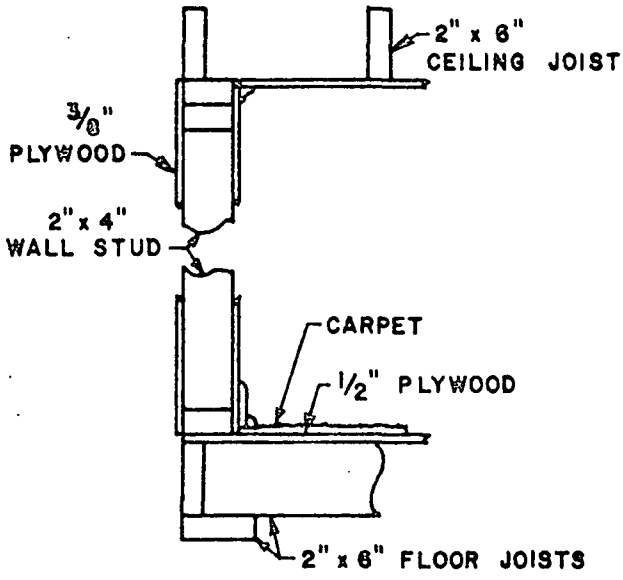

SECT. A-A SCALE: 3/4" = 1'-0"

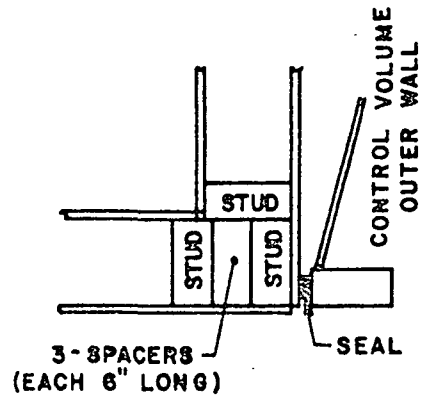

SECT. B-B
SCALE: 1 1/2" = 1'-0"

Figure 3. Test chamber front wall and details

Control Volume

An integral part of the sonic boom simulator is an air-tight chamber, or control volume, that allows a particular wall of the test chamber to be loaded uniformly during a sonic boom. This control volume consists of an outer concave wall, shown in Figure 4, that affixes to one of the walls of the test chamber, as indicated in Figure 1. The concave wall is in the shape of a truncated pyramid and is rigidly constructed so that its deflection would be negligible compared to the test chamber wall. The strength of the concave wall comes from the cross bracing and the thicker plywood used on its inner surface. A circular opening was cut in the vertical center section large enough to provide a one inch clearance around the diaphragm. The edges of the opening were well rounded and smoothed to prevent puncturing the flexible neoprene seal. All seams in the concave wall were caulked and the joint between the outer wall and the test chamber was sealed with an automotive type weather stripping. The concave wall was secured to the test chamber with lag bolts and additionally supported by a foundation. A more permanent mounting would create difficulties if a situation warranted access to the interior of the control volume.

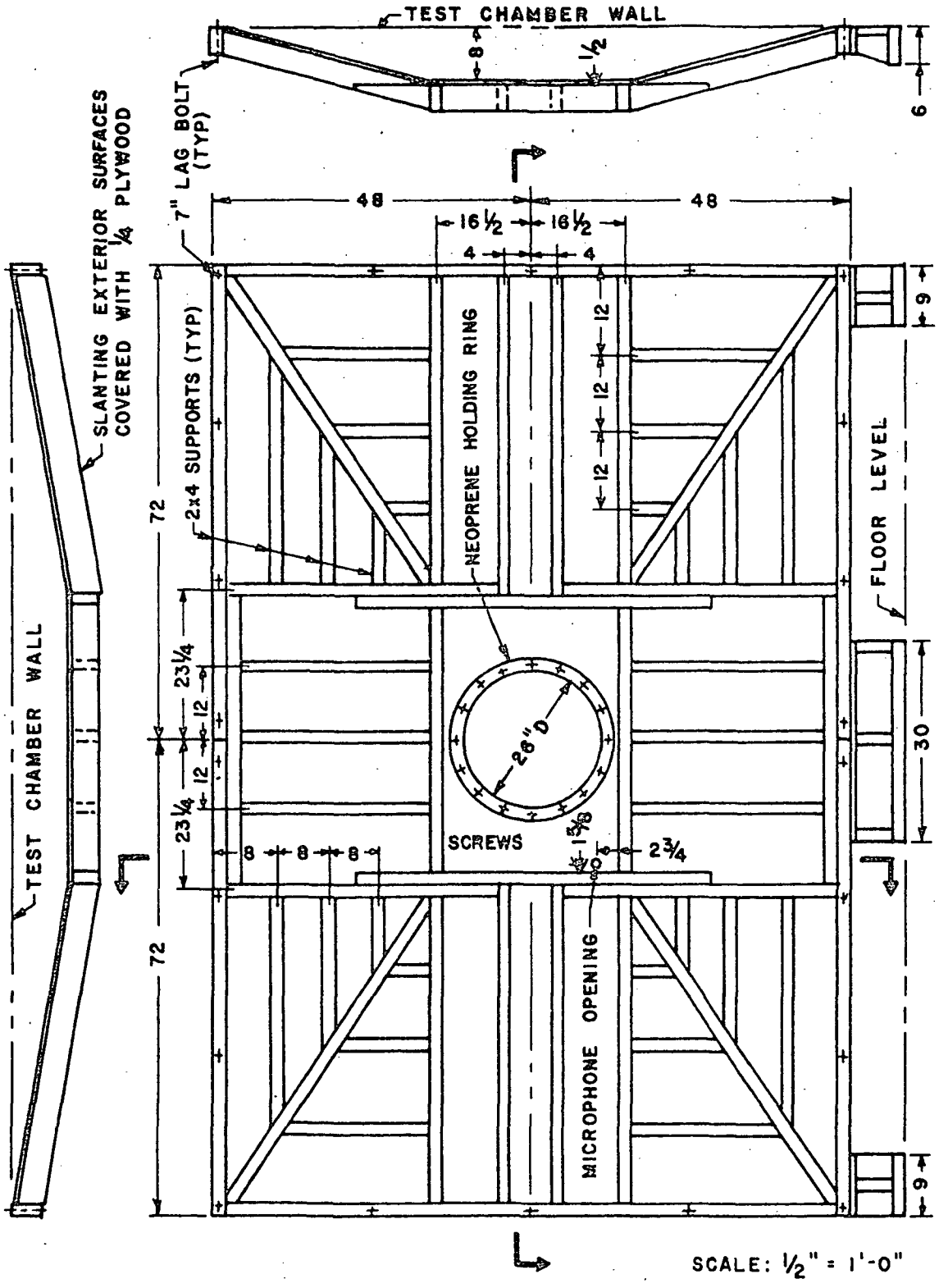

Figure 4. Control volume outer wall

Neoprene Seal

The initial design specified that a neoprene sheet was to be secured to the surface of the diaphragm and to the outer wall of the control volume providing an airtight seal of the chamber. Since the neoprene is attached to the diaphragm, it will follow the same motion as the diaphragm during the simulation of a sonic boom, and it will contribute to the overall weight of the diaphragm subsystem. The force required to provide motion to the subsystem would increase as the overall weight increases, so the weight should be kept to a minimum. The requirements of a neoprene sheet are investigated in Appendix A, and it is determined that the thinnest commercially available sheet would be adequate.

Alterations

During construction the components of the sonic boom simulator, shown in Figure 5, were tested as they were installed to determine if there were any problems that would warrant altering or modifying the original design. The systems that required alterations are as follows:

a. actuating mechanism
b. inertia wheel
c. cam follower pad
d. reservoir pressure reduction.

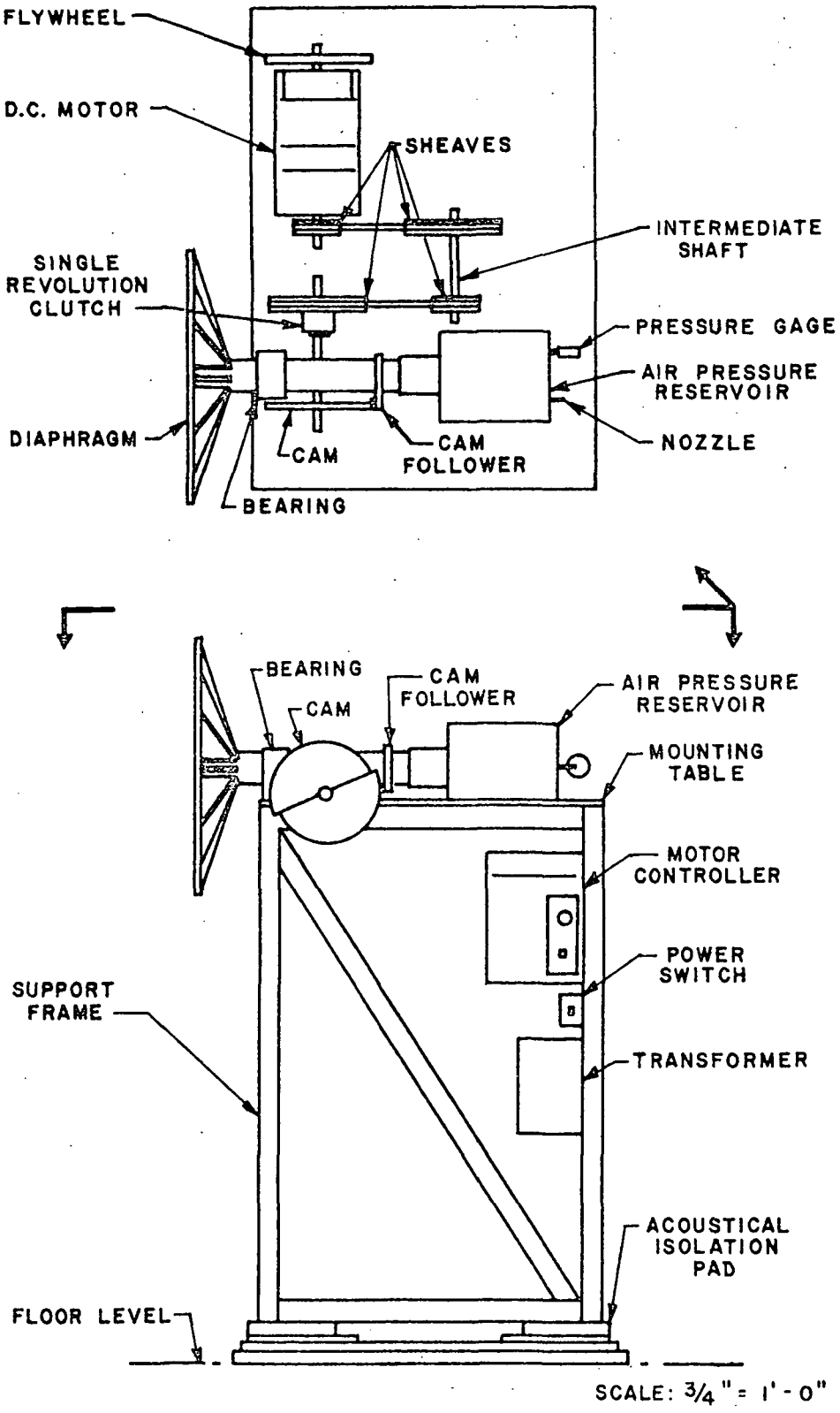

Figure 5. Assembly view of sonic boom simulator

The actuating mechanism consists of a single revolution clutch that is allowed to rotate by energizing a solenoid. If the solenoid remains energized, the single revolution clutch continues to rotate; and since a revolution only takes one quarter of a second, a mechanical tripping device was first developed to prevent more than one revolution. After the solenoid was received, it was found that excessive lateral motion of the solenoid core occurred hampering the operation of the mechanical device. Rather than restrict the solenoid core and decrease its pulling capacity, a more basic approach was tried. If the time that the solenoid was energized could be controlled, the solenoid could be attached directly to a clutch stop lever. Such a momentary contact switch was not commercially available, but a simple electrical switch that could perform the task was developed. A schematic diagram of the circuitry is shown in Figure 6. When the momentary contact switch is in the normally closed position, alternating current from a wall outlet passes through a resistor, limiting the current in the circuit; through a diode, rectifying the current; and into the capacitor. The resistor is a lightbulb and will initially glow as the capacitor is being charged. When it ceases to glow, the capacitor has reached sufficient charge to energize the solenoid. Depressing the momentary contact switch allows the capacitor to discharge through the solenoid, thus permitting the solenoid to only be energized instantaneously. All the electrical components are enclosed in a unit that enable the

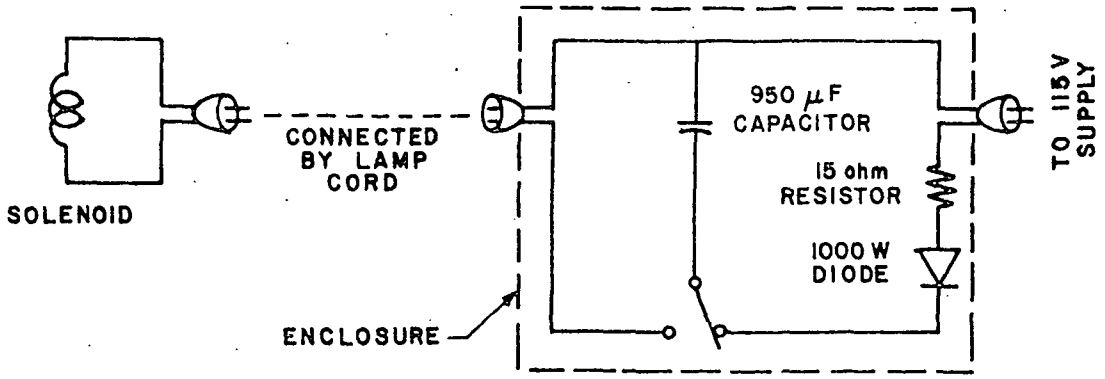

Figure 6. Schematic diagram of electrical switching circuit

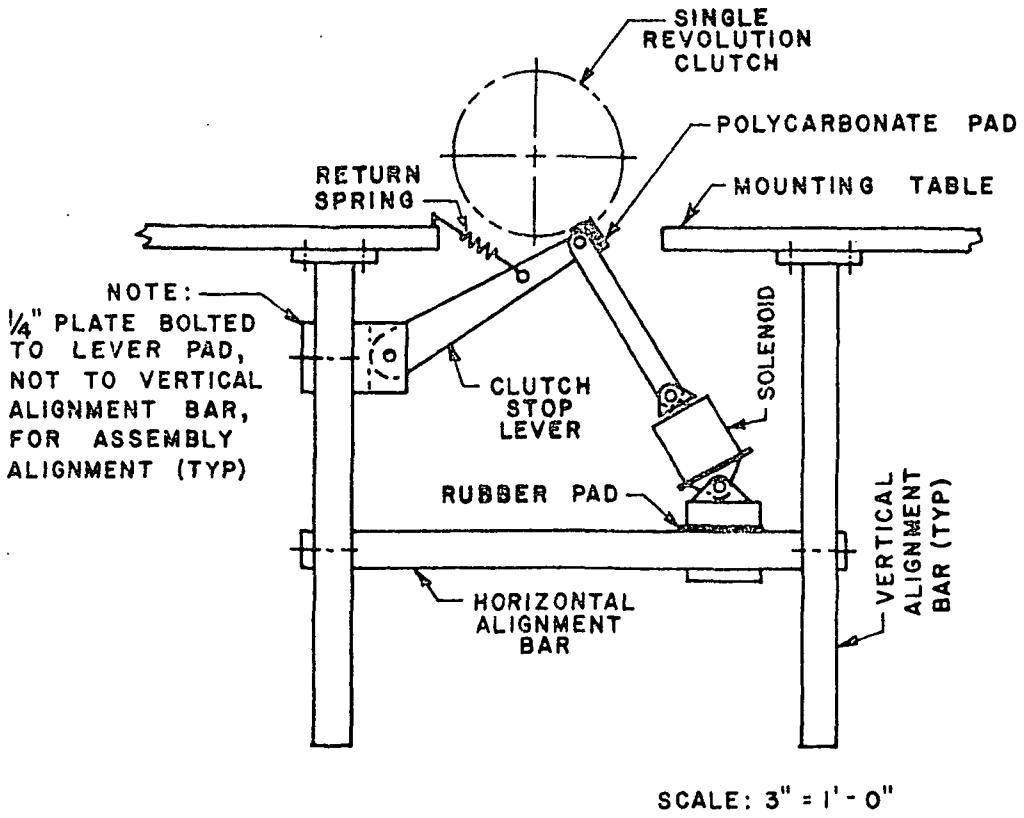

Figure 7. Mechanical actuating mechanism

sonic boom simulator to be operated from the monitoring control side of the test chamber. In Figure 7, the resulting attachment of the solenoid to the clutch stop lever is shown.

The alteration concerned with the inertia wheel, that was mounted on the axle of the electric motor, was a consequence of an unbalance. The motor speed was one of the variables in the simulation of a sonic boom and since one of the desired motor speeds corresponded to a resonant frequency of the inertia wheel, vibration and noise problems resulted. The perimeter of the inertia wheel had been machined concentric to the axle of the motor so the unbalance was contributed to variations in thickness. Since two 1/2 inch steel plates had been used for its fabrication, machining of all four sides to correct the problem would have greatly reduced the inertia. Therefore, a new inertia wheel was made from one inch steel stock and all surfaces were machined smooth. A savings of inertia was accomplished and the unbalance had been corrected.

Another alteration was involved with the mounting of a nylon pad on the cam follower. When the forcing operation of the diaphragm was first tested, the pad that was epoxy glued to the cam follower came off. Examination of the joint indicated that the failure was not a result of the shear force but instead the impact loading. The epoxy had formed a fillet around the pad that was not damaged; so if a normal force could be applied to the pad for the impact loading, the epoxy would still be used for the shear force. A normal force was

applied to the pad by increasing its length and using two small cap head screws to attach it to the cam follower. The correction is shown in Figure 8.

Prior to the performance test of the sonic boom simulator a calculation error was discovered that produced an overdesign of the requirements for the air pressure reservoir. The corrections are shown in Appendix B, and the alteration that resulted was the replacement of the pressure gage. The new gage had a lower pressure range so that the reservoir pressure could be more accurately determined.

Modifications

The alterations produced a change in an existing system, and the modifications introduce improvements through additional features. A list of the modifications with respect to components is listed below:

a. transformer
b. diaphragm alignment slide
c. motor mounts
d. solenoid noise reduction.

A transformer in the power line of the electric motor was a consequence of the new laboratory facilities. The 3/4 horsepower electric motor that provides the torque to the cam was wired for use of a 220 volt supply as was available in the originally intended laboratory. Since the only available power supply in the new laboratory was 115 volts, the transformer was more economical than having the room wired for the

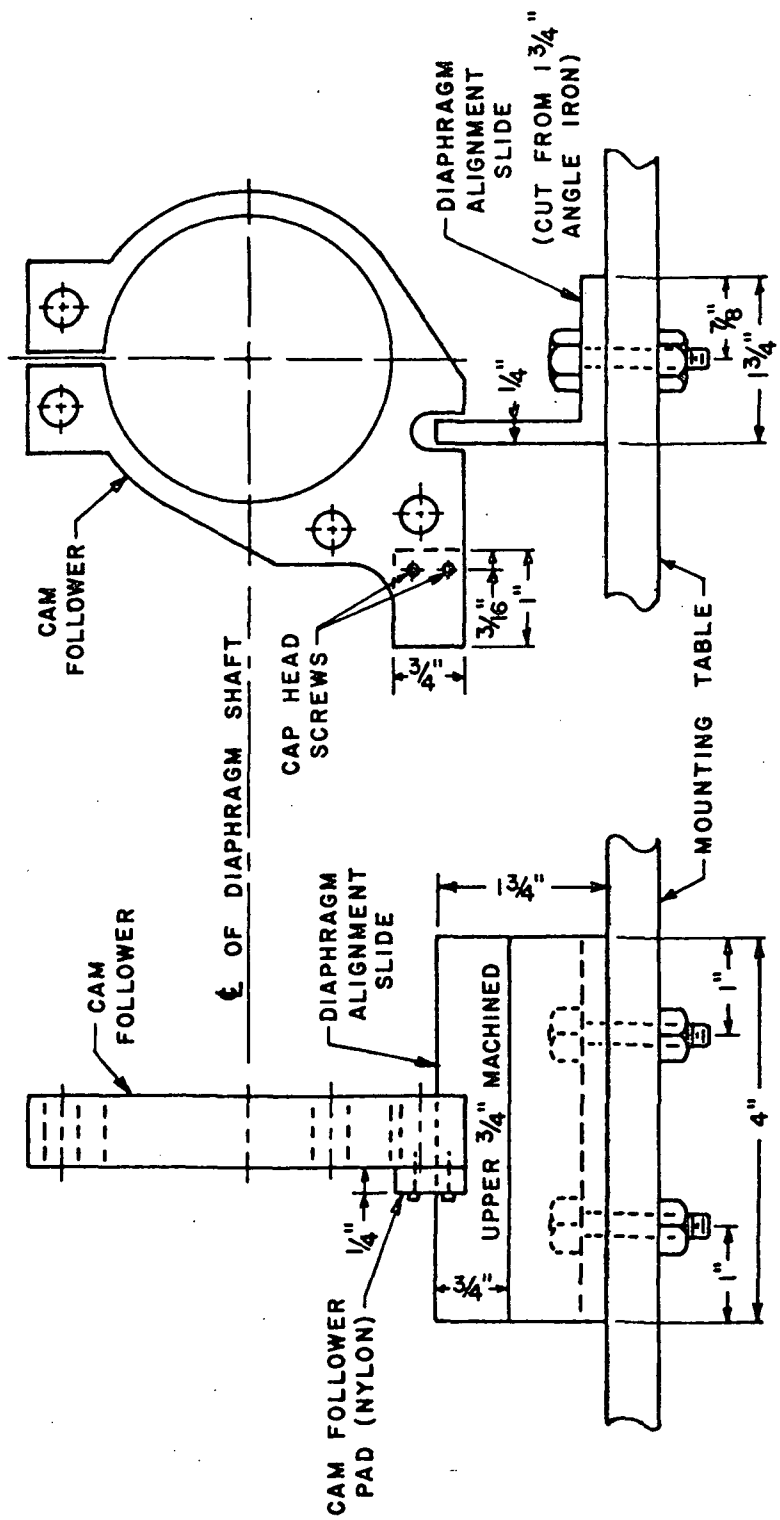

Figure 8. Alignment slide and cam follower pad details

higher voltage. The transformer was located out of the way beneath the mounting table and secured to the support frame, as is shown in Figure 5.

Addition of the diaphragm alignment slide was a precautionary measure to prevent rupture of the neoprene sheet by rotation of the diaphragm. Friction from the cam follower sliding on the cam would produce a rotational force and the only resultant force would have to come from the neoprene sheet. The slide was a piece of 1-3/4 inch angle iron with one arm bolted to the mounting table and the other arm fitted into a slot cut in the lower extreme of the cam follower, shown in Figure 8.

The next modification was the addition of a rubber motor mount for the electric motor. Sixty-cycle noise was being produced by the electric motor and transmitted to the mounting table causing other components to produce noise. To reduce the overall noise level, the transmission path was broken by placing a special rubber pad between the motor and the mounting table and by using rubber washers when bolting the motor to the table. Although the motor still produced some noise, the overall operational noise was lowered.

The fourth modification also dealt with noise reduction but was concerned with the solenoid. Noise would result from the metal to metal impact of the core striking the casement when the solenoid was energized and from the return spring oscillating when the solenoid was de-energized. The relevant components are shown in Figure 7. The first problem was

solved by placing rubber cushions between the contact points to absorb part of the energy from the impact. Vibration of the spring was eliminated by placing a small piece of the neoprene, rolled up, within the spring. An additional reduction was made by mounting the solenoid on a rubber pad to prevent it from transmitting vibrations to any other component.

Reservoir Pressure Corrections

When the air pressure reservoir was initially pressurized, an air leak was evident. The location of the leakage was detected by the application of a soap and water solution that resulted in the escaping air producing bubbles. The only significant leak was due to scratches on the surface of the diaphragm shaft that were corrected by refinishing the surface. Other small leaks were correctable through adjustment.

Acoustic Enclosure

To reduce the ambient noise level in the laboratory, the initial design called for the sonic boom simulator to be covered by an acoustic enclosure. The overall dimensions were specified, but the details had to be worked out. For low frequency sound absorption a high density fiber board was chosen, and to keep the sound pressure from increasing inside the chamber due to reverberation, the interior was covered with an acoustic tile, as shown in Figure 9. A construction

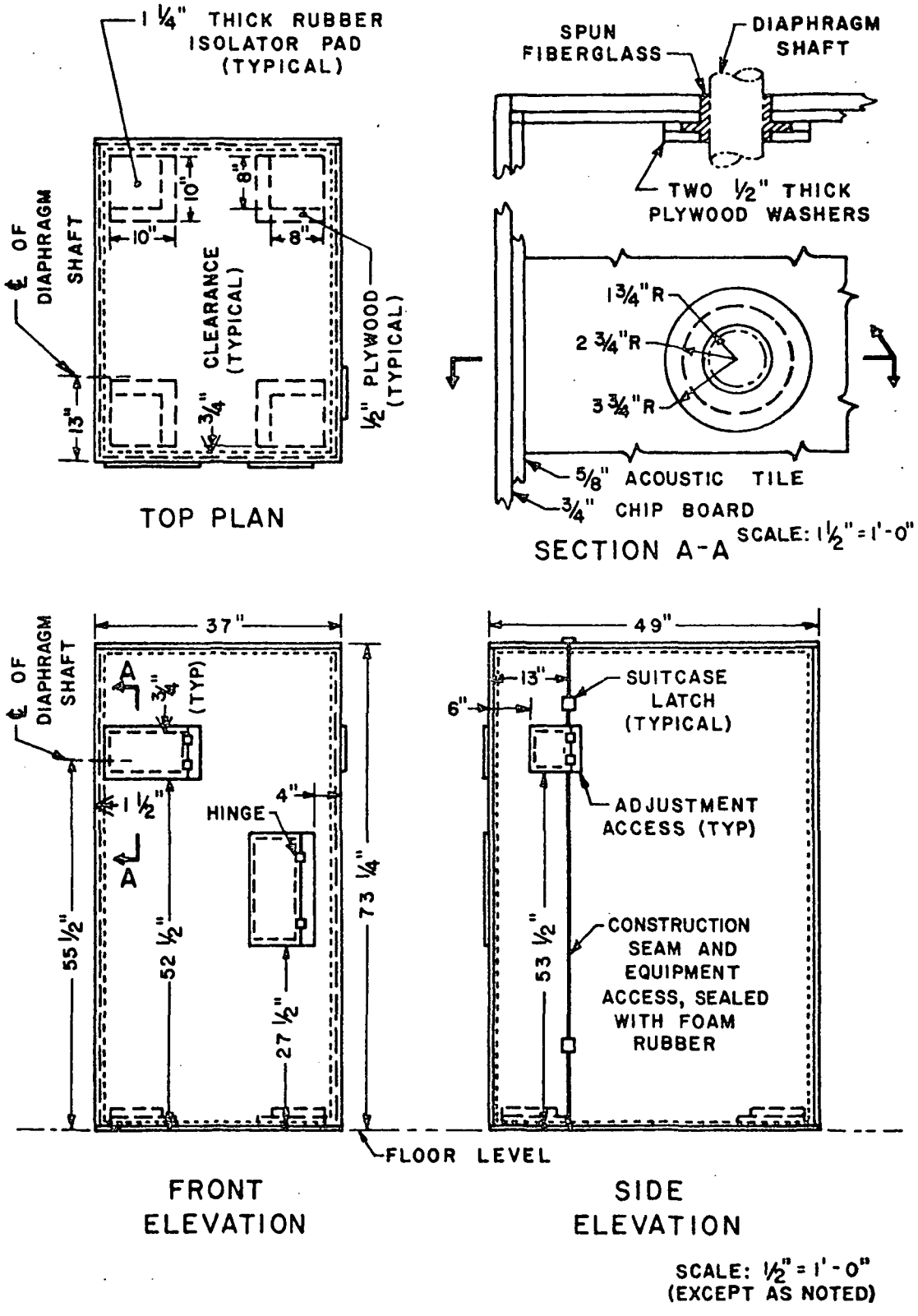

Figure 9. Acoustic enclosure

seam was offset from the center so that one end of the enclosure could be removed for maintenance of the simulator. Foam rubber is used for a seal in the joint, and suitcase latches secure the sections together. The opening around the diaphragm shaft was extended with wooden washers, cut from plywood, to allow the clearance about the diaphragm shaft to be filled with spun fiber glass. The enclosure rests on the floor and has an acoustical isolation foundation between it and the mounting table. The acoustical isolation foundation was placed on the acoustic tile lining with the plywood distributing the load over a larger area and the rubber absorbing the vibrational energy. An additional requirement of the foundation that was considered was proper height for the mounting table to provide vertical alignment of the diaphragm to the clearance opening in the control volume.

Completion of Construction

The finalization of the construction of the sonic boom simulator was sealing the connection of the diaphragm to the control volume outer wall. The neoprene sheet was epoxied to the diaphragm and secured to the control volume outer wall with a holding ring shown in Figure 4. The control volume was then airtight and with all systems properly operating, the sonic boom simulator was ready to be tested.

TESTING AND EVALUATION

Performance Test and Corrections

Prior to the presentation of the testing of the sonic boom simulator, a more detailed examination of the sonic boom phenomena may be helpful to the reader. As mentioned in the introduction, a sonic boom is a pressure disturbance that is produced by a supersonic aircraft. The pressure signature is rather complex near the aircraft, as shown in Figure 10, but evolves into a simpler wave as the distance from the aircraft increases. The rough peaks near the aircraft are produced by any abrupt change in the contour of the aircraft, and the smoothness occurs as an effect of the atmosphere during propagation to the ground. The pattern in the far field resembles an N-shaped time history and is of greatest interest since it is for an aircraft in a normal high altitude flight configuration. This wave is characterized by a sudden pressure rise, ΔP, followed by a linear decay to a pressure below atmospheric, $-\Delta P$, and another sudden rise in pressure back to normal. The time required for the first pressure rise is generally referred to as the rise time, t, and the period for the N-impulse is the duration, D. An actual sonic boom only approaches this idealized N-wave, but the differences, depending on the temperature, pressure, and wind currents of the atmosphere, are usually small.

The instrumentation for the test had to be capable of measuring low frequencies since sonic booms range from

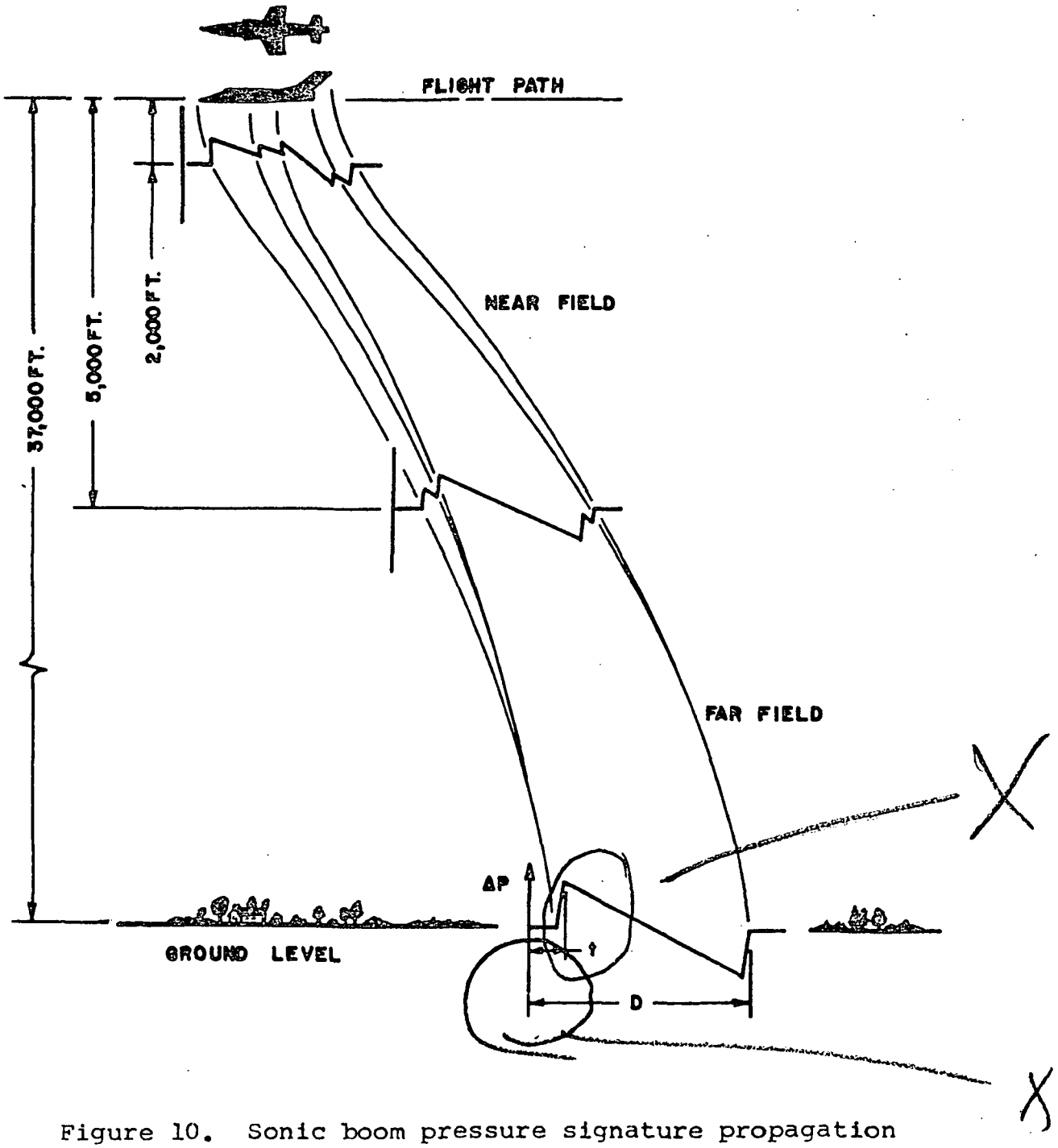

Figure 10. Sonic boom pressure signature propagation

2.5 hertz up to 25 hertz, that is, durations of 0.04 to 0.4 seconds. The components utilized in the instrumentation are listed below:

a. one inch microphone
   Brüel and Kjaer type 4146
b. microphone carrier system
   Brüel and Kjaer type 2631
c. storage oscilloscope
   Tektronix type 549
d. camera with oscilloscope mount
   Tektronix type C30A.

The microphone carrier system with the one inch microphone has a frequency range from 0.1 hertz to 18 kilohertz, which was more than adequate for the test. The oscilloscope gave an immediate visual display of the pressure signature and the camera provided a permanent record of the data.

The test was performed by sealing the microphone in a one inch diameter hole that was drilled in the outer wall of the control volume as shown in Figure 4, and observing the trace of the pressure change on the oscilloscope screen during the simulation of a sonic boom. To determine the performance, the overpressure, rise time, and duration were increased by increasing the cam offset, decreasing the reservoir pressure, and decreasing the motor speed, respectively. The effect of decreasing the motor speed and reservoir pressure are shown in Figures 11 and 12.

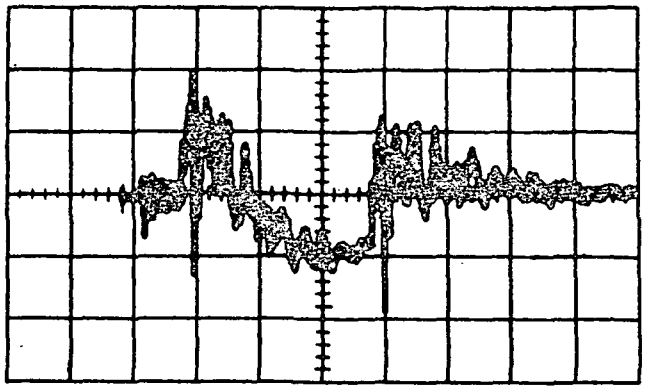

Figure 11. Oscilloscope trace of correctable pressure signature A. One division vertically = 0.5 psf. One division horizontally = 0.05 second

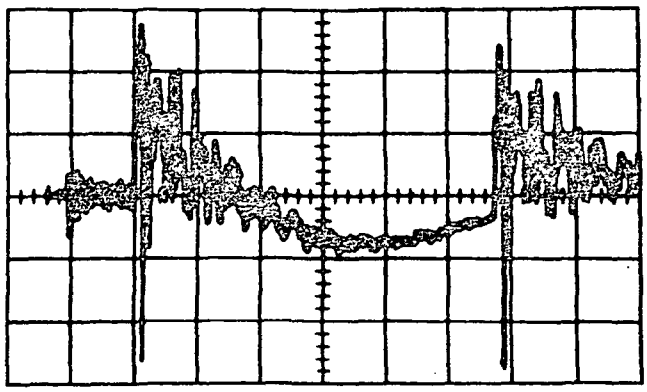

Figure 12. Oscilloscope trace of correctable pressure signature B. One division vertically = 0.5 psf. One division horizontally = 0.05 second

As a result of the test, two problems were exposed that required corrective measures, one was oscillations that were superimposed on the N-wave, and the other was a nonlinear pressure decay. The oscillations are apparent in both Figures 11 and 12 and were assumed to be the product of vibrations that either entered the diaphragm or were produced by it. To decrease the vibration that was emanating from the diaphragm face plate, a sound dampening material was added between the reinforcement ribs. To decrease the separation of the cam follower from the cam, which would have produced oscillations of the entire diaphragm system, a shock absorber was attached to the cam follower and bolted to the mounting table, as shown in Figure 13. To reduce any transmission from the metal to metal contact of the clutch stop lever with the single revolution clutch, a nylon pad was mounted on the clutch stop lever. This nylon pad later had to be replaced with one made from polycarbonate due to the nylon not being capable of withstanding the impact loading of stopping the single revolution clutch.

The nonlinear pressure decay is more noticeable in Figure 12, and an analysis of the driving system for the cam, as in Appendix C, was made to determine the cause. Power is transmitted from the d.c. motor to the cam by means of V-belts and sheaves, which were found to be operating below their power conveying capacity, thus producing a power fade during the simulation of a sonic boom. The power

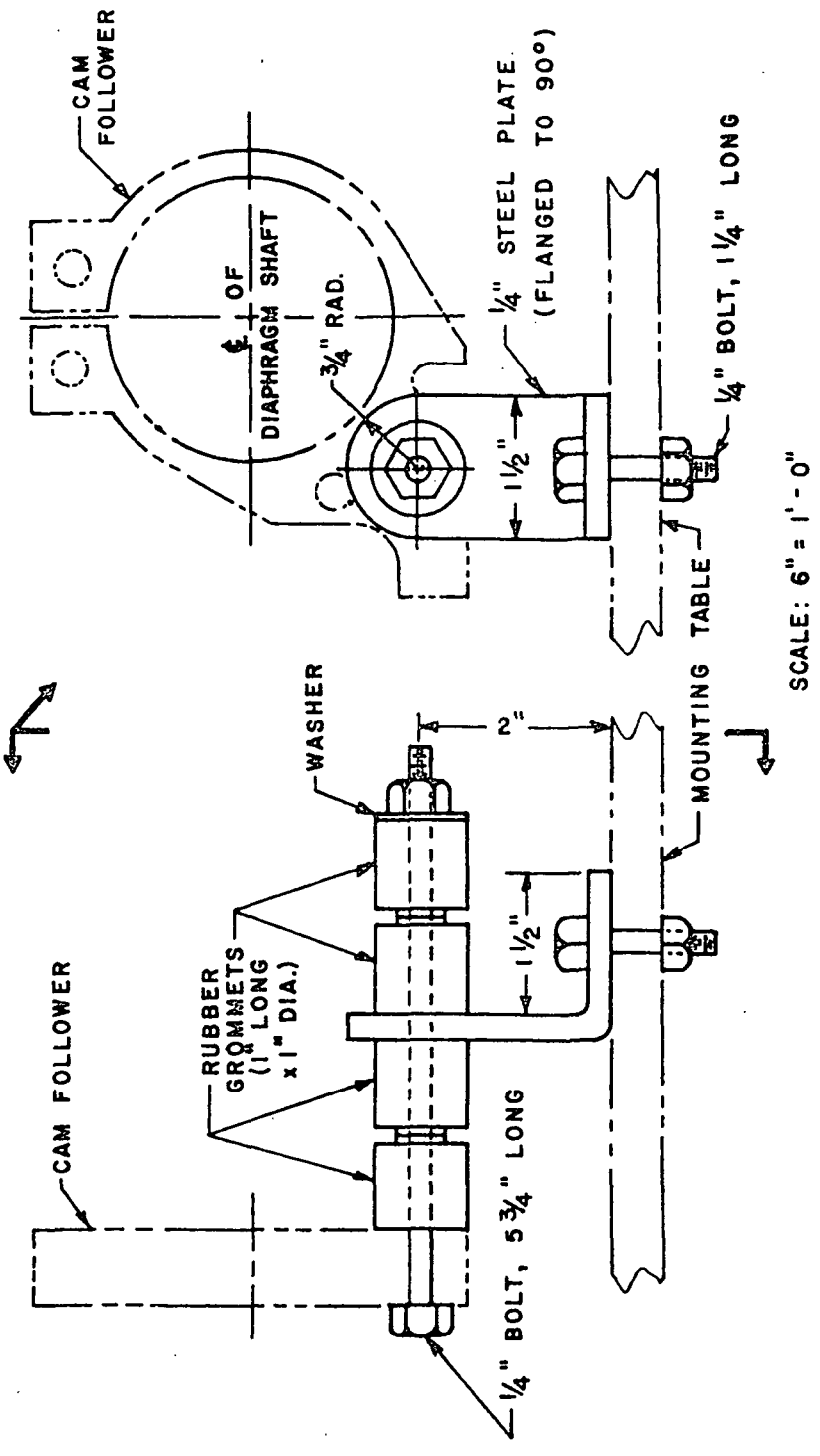

Figure 13. Shock absorber detail

transmission ability was increased by changing to double V-belts and larger sheaves.

The improvements of the pressure signature are shown in Figures 14 and 15 in that the oscillations are significantly reduced and that the pressure decay is approaching linearity. The pressure decay would never be perfectly linear due to the circular cam producing a sine wave pattern, but the proximity is sufficient.

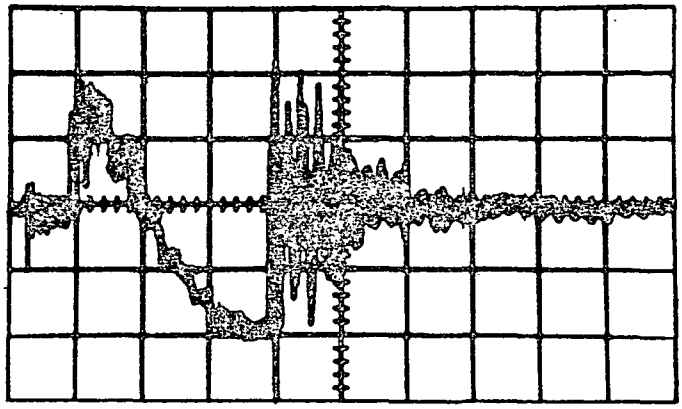

Figure 14. Oscilloscope trace of pressure signature A. One division vertically = 0.5 psf. One division horizontally = 0.05 second

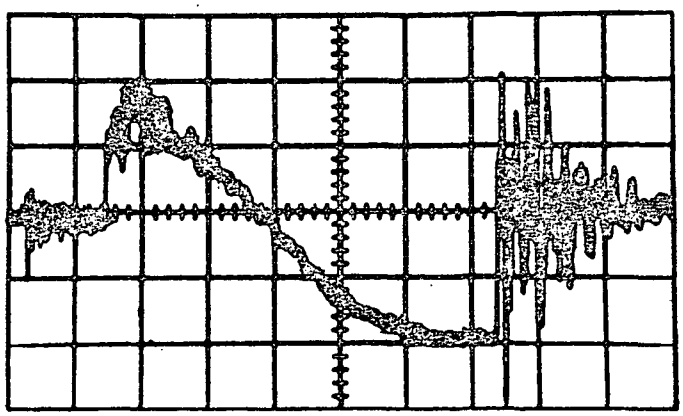

Figure 15. Oscilloscope trace of pressure signature B. One division vertically = 0.5 psf. One division horizontally = 0.05 second

Calibration Test

The intention of the calibration test was to associate simulator adjustments with pressure signatures and with aircraft. This was accomplished by utilizing the same instrumentation as in the performance test to obtain photographs that indicated the effect of the variable adjustments. The pressure signatures thus obtained were idealized to an N-waveform by defining the rise time as the time required for the overpressure to reach a maximum; the overpressure as the mean value of the oscillations, and the duration as the sum of twice the rise time plus the time required for a complete reversal of overpressure. The method of dimensionalizing the pressure signatures is illustrated in Figure 16. The rise

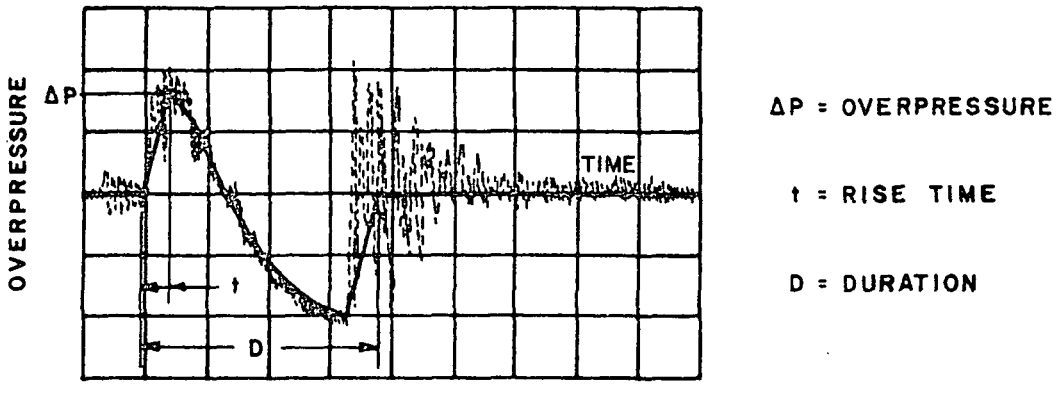

Figure 16. Idealized pressure signature

time and the duration are readily determined since the divisions of the horizontal scale are in milliseconds, but the overpressure required a conversion from volts to pounds per square foot. The conversion was obtained by using a pistonphone, Brüel and Kjaer type 4220, that produced a known input, and by information from Beranek (2) that gave a correspondence of one pound per square foot for a two volt indication on the vertical scale of the oscilloscope.

The simulator was designed such that each of the boom parameters could be varied independently by measurable adjustments of the simulator. That is, the duration is related to the motor speed, which depends on a scaled controller setting; the rise time corresponds to the reservoir pressure, which is goverened by a pressure gage; and the overpressure is associated with the cam offset, that can be measured in fractions of an inch. The effects of the adjustments are illustrated as follows: durations of 0.16 and 0.31 seconds are shown in Figures 14 and 15 for controller settings of 5 and 3.5; rise times of 0.05 and 0.025 seconds are shown in Figures 17 and 18 for reservoir pressures of 20 and 15 pounds per square inch; and overpressures of 0.6 and 1.2 pounds per square foot are shown in Figures 18 and 19 for cam offsets of 0.12 and 0.19 inches, all indicated respectively. The reproducibility and variability of the simulations are apparent in the above mentioned figures, and with similar photographs, the curves in Figures 20 and 21 were developed to show durations and overpressures as functions of the adjustments. The

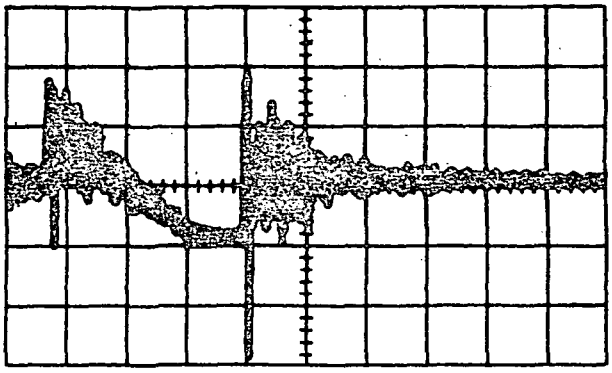

Figure 17. Oscilloscope trace of pressure signature C. One division vertically = 0.5 psf. One division horizontally = 0.05 second

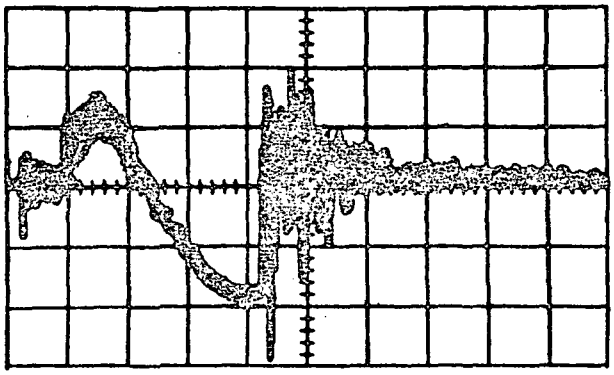

Figure 18. Oscilloscope trace of pressure signature D. One division vertically = 0.5 psf. One division horizontally = 0.05 second

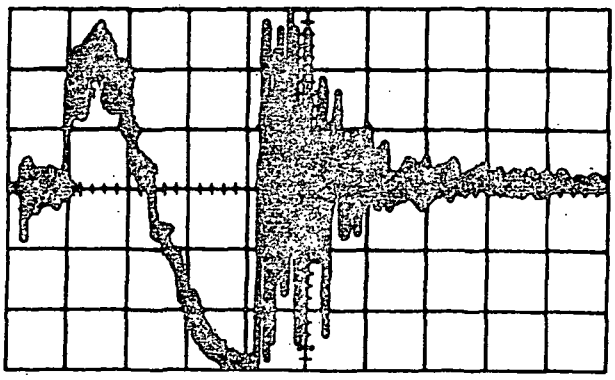

Figure 19. Oscilloscope trace of pressure signature E. One division vertically = 0.5 psf. One division horizontally = 0.05 second

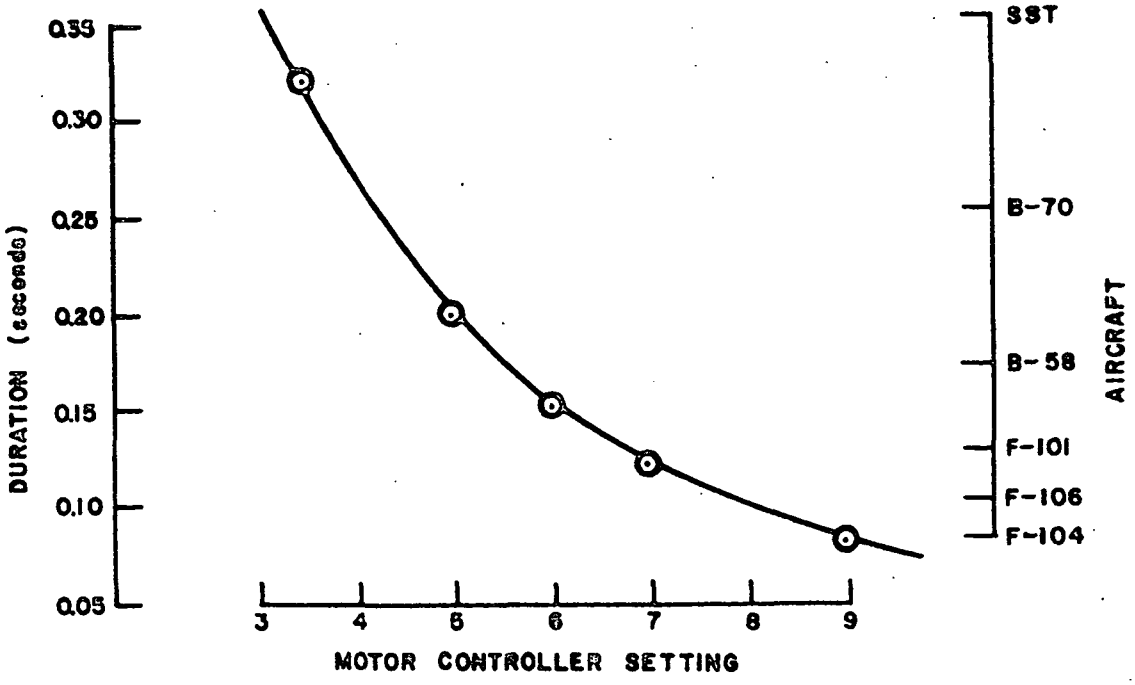

Figure 20. Correlation of motor controller setting with duration and aircraft

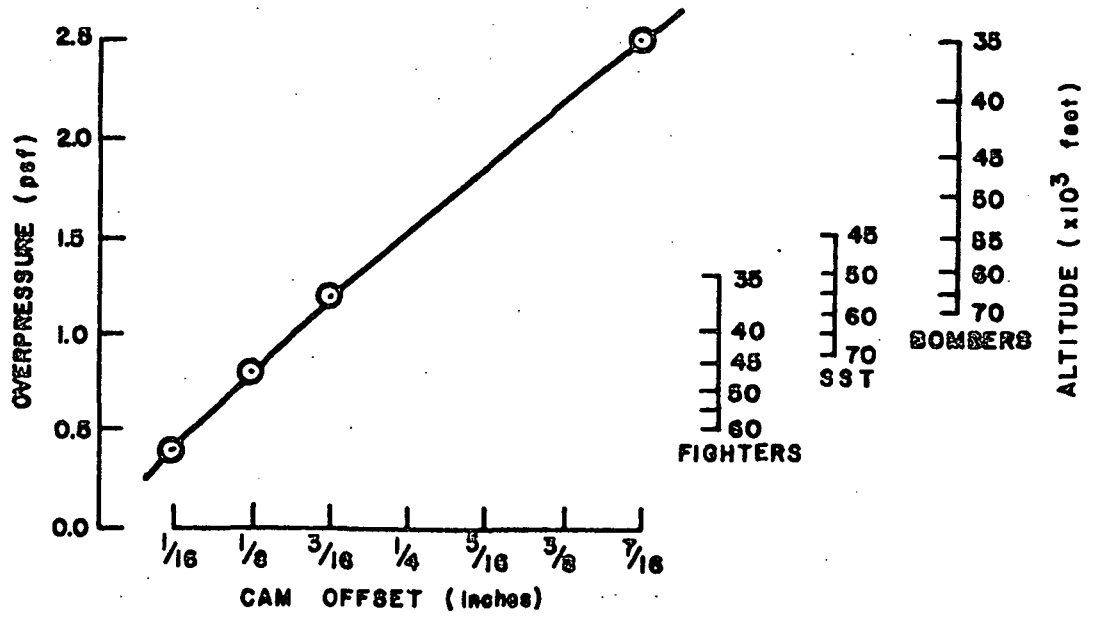

Figure 21. Correlation of cam offset with overpressure and aircraft altitude

rise time was too dependent on the cam offset and the shock absorber for a correlation with the reservoir pressure, but ranges from 0.005 to 0.030 seconds were established which are in agreement with the design specifications. The curves in Figures 20 and 21 enable the simulator to be set for simulations of a predetermined duration and overpressure simply by adjusting the motor controller and the cam offset to the designated settings.

To relate the simulated sonic boom with aircraft required a generalization, in that the atmosphere affects the parameters of booms, produced by aircraft, in varying degrees. The duration is least affected and can more readily be related. Information from Young (11) gave typical durations for aircraft and are indicated in Figure 20 so that the simulator can be set for a duration that corresponds to a particular aircraft. The overpressure is apparently affected by altitude as much as it is by aircraft configuration. Average values of the overpressure were determined by information from previous research (7) as functions of altitude for three types of aircraft. The results are related to the cam offset of the simulator by the curve in Figure 21. The rise time is so dependent on atmospheric conditions that no parallel could be drawn between the simulator and aircraft. According to (10), identical rise times are available from different types of aircraft, and they range from 0.001 to 0.030 seconds. The only comparison that can be made is that the 0.005 to 0.030

second rise times obtainable from the simulator are in agreement with those of aircraft.

It is apparent from Figures 20 and 21 that the simulator meets the design specifications of the initial design, and that it is producing simulations that are comparable to those associated with aircraft.

Evaluation

It has been suggested by Young (11) that a better comparison of sonic booms is made by analyzing the energy distribution in frequency bands rather than by associating the characteristic parameters of the N-waves. Although the previous correlations can still be used to relate the simulations with particular aircraft, an analysis was made to show that the simulator does in fact produce a simulation which agrees with theoretical and aircraft produced N-waves.

To determine the energy distribution in frequency bands, or generally referred to as the energy spectral density, a simulated sonic boom was recorded and then played back through a filter. The advantage of the recording was that the playback speed could be changed enabling the energy in lower frequencies to be determined. To complete the formal list of instrumentation, the following components were used in addition to those in the performance test:

a. frequency modulation tape recorder
   Brüel and Kjaer type 7001
b. audio frequency spectrometer
   Brüel and Kjaer type 2112
c. extension filter set
   Brüel and Kjaer type 1620.

The simulated sonic boom was recorded on magnetic tape at 6 inches per second and then played back at 60 inches per second for the lower frequency analysis. Thus when the playback speed was returned to the normal 6 inches per second, a

full spectrum was obtained for the center frequencies from 1.25 to 1250 hertz. The center frequencies are with respect to the one-third octave bandwidth that was the mode of operation of the filter for the analysis. For a pressure level indication in the bandwidths, an attempt was first made to use a graphic level recorder to provide a permanent record of the readings, but its operation was unsatisfactory. A rapid response was required for the impulsive indications, and the inertia of the writing pens suppressed this movement. The oscilloscope appeared to be the only available means of collecting the data and so by double checking each reading, reliability in the data was assured.

The data obtained was pressure levels associated with bandwidths and required a conversion to energy spectral density. Information by von Gierke (7) gives the following description:

$$\left|P(w)\right|^2 = \frac{\Delta P^2}{\Delta f} \tag{1}$$

which in terms of decibels would be

$$10 \log \left|P(w)\right|^2 = 10 \log\left\{\frac{\Delta P^2}{\Delta f}\right\} \text{dB}. \tag{2}$$

Plotting the energy spectral density against the center frequencies yields the curve shown in Figure 22. The spike at 63 hertz and the surrounding increase is attributed to the motor noise that is developed by the simulator and would tend to make the simulation seem louder than a comparable actual boom. For comparison, the theoretical energy spectral density based on Fourier integral techniques is shown in

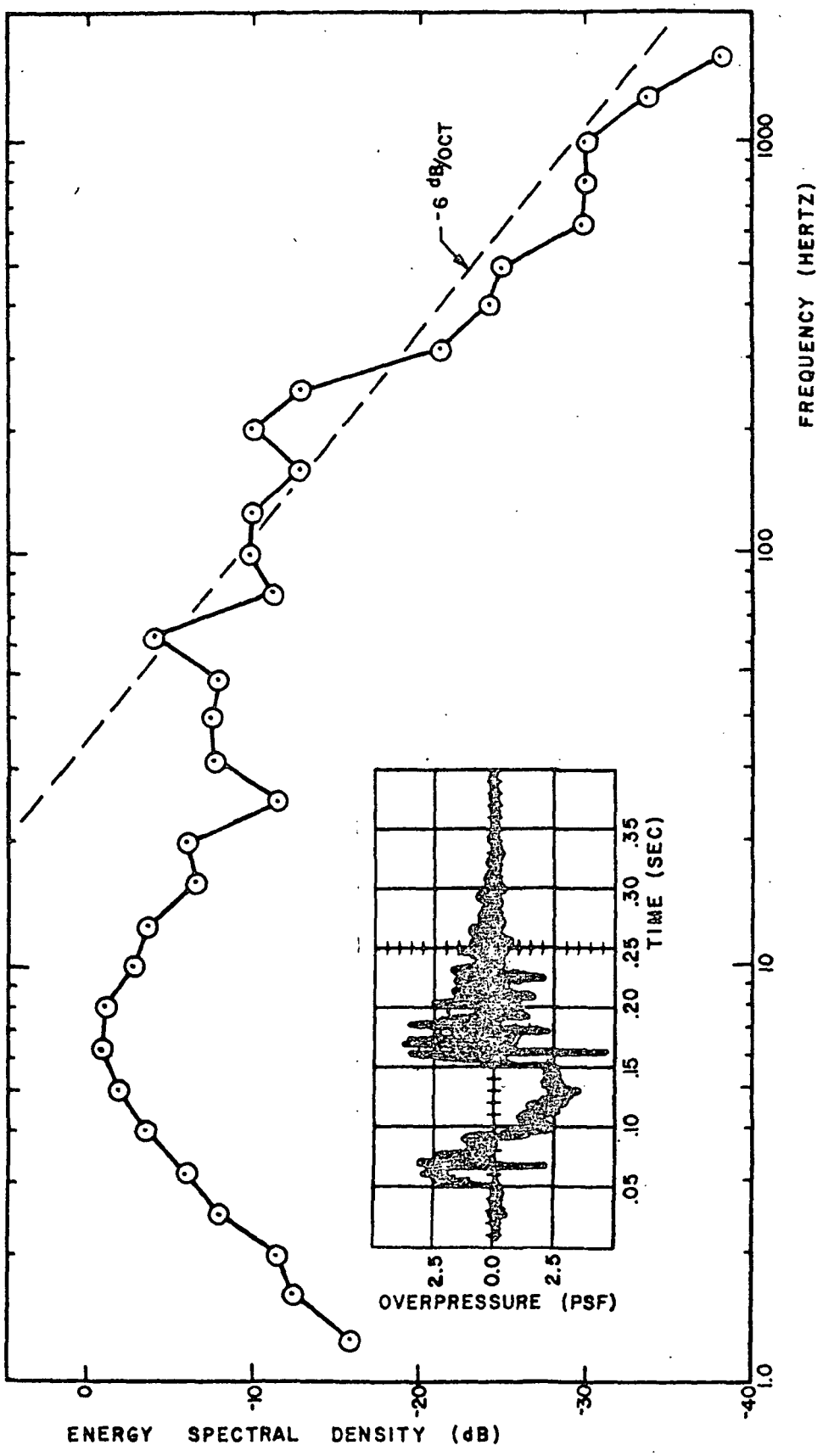

Figure 22. Energy spectral density for a simulated N-wave

Figure 23, as indicated by von Gierke (7), and the actual energy spectral density as measured for a supersonic aircraft (10) is shown in Figure 24. It should be noted that for all three figures the energy reaches a maximum below 10 hertz, and that the energy decreases by 6 decibels per octave for the upper frequencies. This means that the major portion of the energy is contained in the subaudible frequencies, and that the simulation is in agreement with both theory and fact.

Since the simulator is to be used later in sleep study experiments, a measure of the operating noise may prove to be a useful part of the evaluation. A sound level survey kit, Brüel and Kjaer type 2204, was used to obtain the sound levels within the test chamber both with and without the simulator operating. The results are indicated in Figure 25 and show that the levels are higher in the lower frequencies. Although there is a noticeable increase, the concentration in the lower frequencies is an advantage. The human auditory system attenuates the lower frequencies making such noises less distracting and acceptable for sleeping conditions.

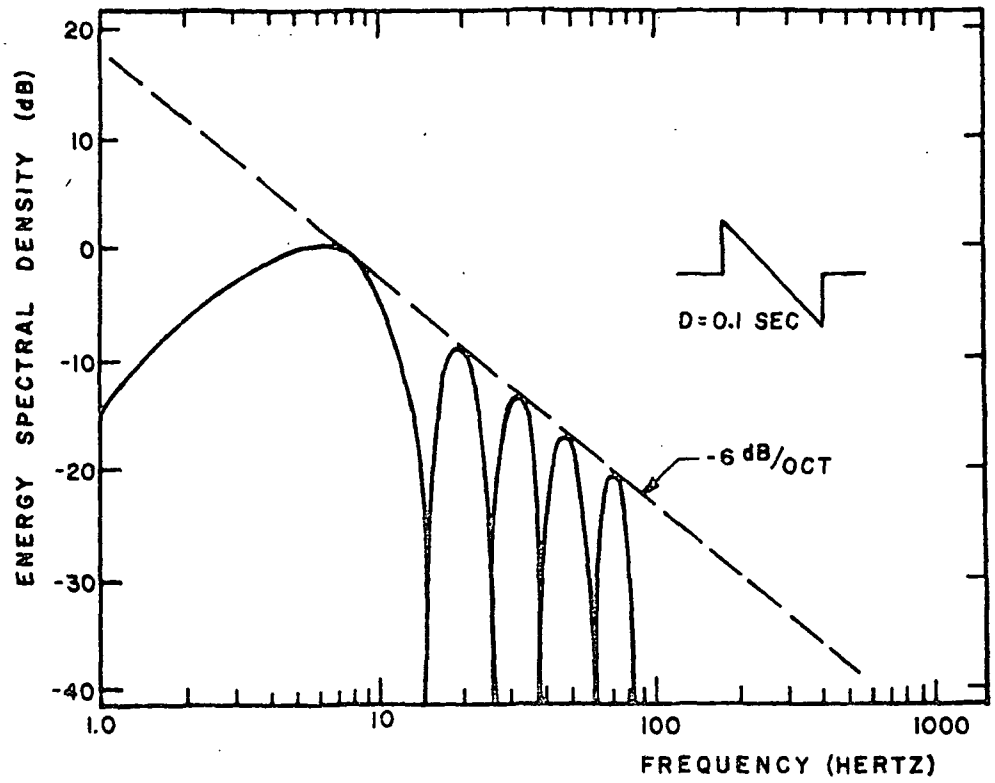

Figure 23. Energy spectral density for an ideal N-wave

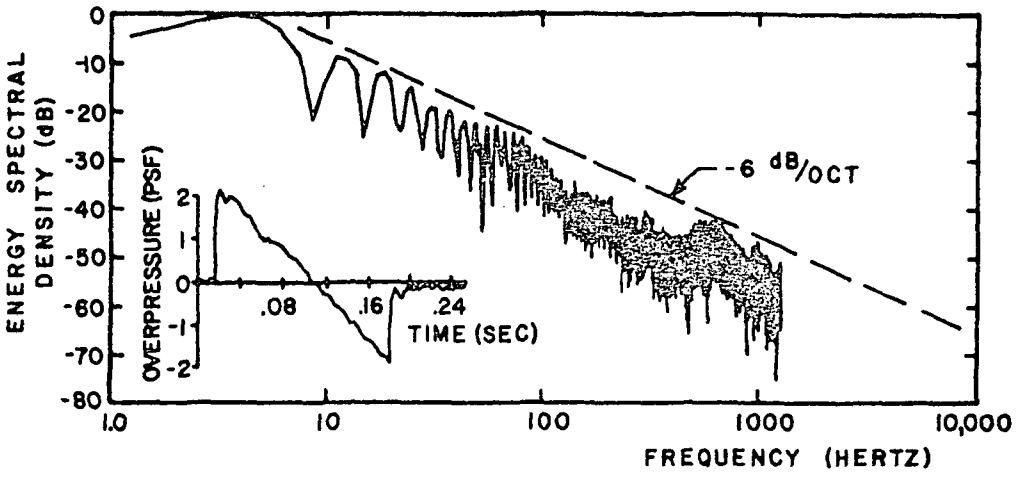

Figure 24. Energy spectral density for an N-wave produced by a supersonic aircraft

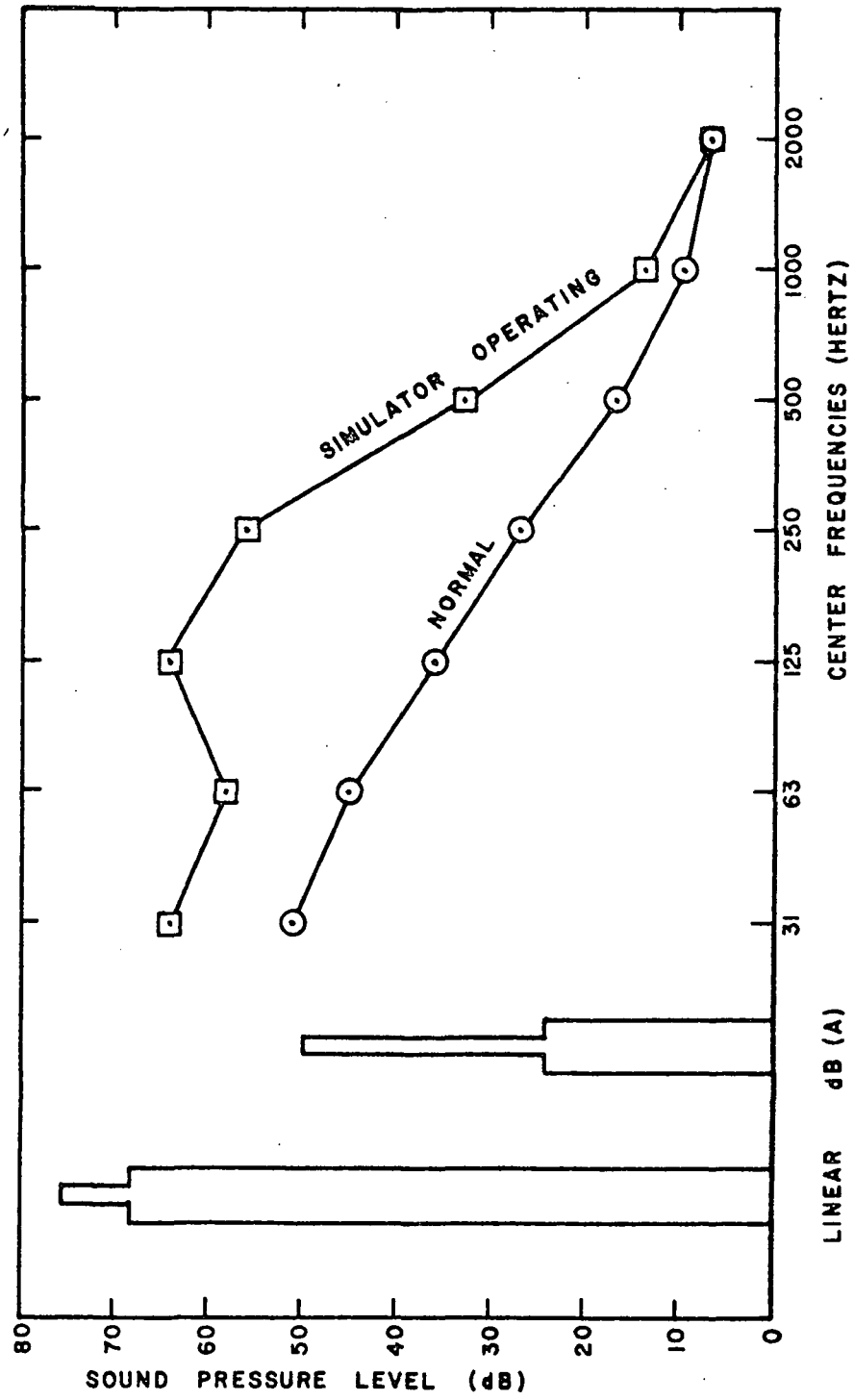

Figure 25. Ambient noise levels inside test chamber

SUMMARY

The sonic boom simulator, along with the acoustical test chamber, provides the best means of conducting accurate experimentation on the physiological effects of sonic booms. The simulator produces the effects of sonic booms with rise times between 0.005 and 0.030 seconds, durations between 0.08 and 0.35 seconds and overpressures between 0.4 and 2.5 pounds per square foot. Variation of each boom parameter can be accomplished by independent adjustments of the simulator and with a minimum of effort.

Analysis of the simulations, with respect to the energy spectral density, indicated that the sound energy distribution was comparable to plots for an ideal N-wave and for actual supersonic aircraft.

LIST OF REFERENCES

1. Baumeister, T., and L. S. Marks. 1967. Standard Handbook for Mechanical Engineers. 7th Edition. McGraw-Hill Book Company, New York.

2. Beranek, L. L. 1960. Noise Reduction. McGraw-Hill Book Company, New York.

3. Browning Power Transmission Equipment, Browning Catalog No. 5. 1968. Browning Manufacturing Company, Maysville, Kentucky.

4. Hubbard, H. H. 1971. Aerospace vehicle noise-induced structural vibrations. Sound and Vibration 5(12): 14-17.

5. Juvinall, R. C. 1967. Engineering Considerations of Stress, Strain, and Strength. McGraw-Hill Book Company, New York.

6. Lukas, J. S., and K. D. Kryter. 1968. A preliminary study of the awakening and startle effects of simulated sonic booms. National Aeronautics and Space Administration. Contractor Report No. 1193. Langley Research Center, Virginia.

7. Proceedings of the sonic boom symposium. 1966. Journal of the Acoustical Society of America 39(5):S1-S73.

8. Redman, L. W. 1970. Engineering analysis and design of a mechanism to simulate a sonic boom. Unpublished Masters thesis, Department of Mechanical and Aerospace Engineering, North Carolina State University at Raleigh.

9. Shigley, J. E. 1963. Mechanical Engineering Design. McGraw-Hill Book Company, New York.

10. Sonic boom experiments at Edwards Air Force Base. 1967. National Sonic Boom Evaluation Office, Arlington, Virginia. Interim Report No. NSBEO-1-67:C-I-1 - F-1.

11. Young, J. R. 1966. Letters to the editor - energy spectral density of the sonic boom. Journal of the Acoustical Society of America 40(2):496-498.

A P P E N D I C E S

Appendix A. Design Analysis of Flexible Neoprene Seal

The thickness of the neoprene sheet can be determined by examining the stresses in a segment on the surface of the diaphragm, and then checked by finding the deflection at the clearance space between the diaphragm and the control volume outer wall. The segment on the surface is taken which covers one of the one-eighth inch diameter holes that was drilled for weight reduction. The external forces consist of an assumed simple support about the boundary of the opening and of a distributed load produced by acceleration and chamber pressure. The loading due to acceleration can be determined by Newton's Second Law,

$$F = ma \tag{3}$$

The distributed load is found by dividing (3) by the area of the diaphragm.

$$w_a = \frac{ma}{A} \tag{4}$$

The mass would be for the weight of the neoprene, which is the product of the density and the volume, and the acceleration would be for the displacement and rise time of the simulator. Substituting in (4)

$$w_a = \frac{1}{A} \frac{\rho AT}{g} \frac{2d}{t^2} \tag{5}$$

ρ = 0.034 pounds per cubic inch

d = 0.11 inch

g = 386 inches per square second

t = 0.005 seconds.

Therefore:

$$w_a = \frac{0.034 \times T \times 2 \times 0.11}{386 \times 0.005^2} = 0.705T \text{ psi} \quad (6)$$

The loading due to chamber pressure would simply be the over-pressure

$$w_o = 3.0 \text{ psf} = 0.021 \text{ psi} \quad (7)$$

The total distributed load, by superposition, would be the sum of equations (6) and (7).

$$w = 0.705T + 0.021 \text{ psi} \quad (8)$$

The thickness of the neoprene sheet can be determined from the equation presented by Baumeister and Marks (1)

$$S = \frac{kr^2}{T^2} w \quad (9)$$

$S = 500$ psi

$k = 1.24$

$r = 1/16$ inch.

Solving for the thickness

$$500 = \frac{1.24 (0.705T + 0.021)}{16^2 T^2}$$

$$500 T^2 - 0.0034T - 0.0001 = 0$$

$$T = 0.00045 \text{ inch}$$

As indicated in equation (9), the stress is inversely proportional to the thickness. Therefore, an increase in thickness would result in less stress in the neoprene. Since 1/64 inch is the minimum thickness that is commercially available, it can be used and the stresses developed would be acceptable.

To determine the deflection at the clearance space, the inertial load was assumed to decrease linearly from the diaphragm to the control volume outer wall. Thus, the distributed load as described by equation (8) would be

$$w = \frac{0.705}{2}\left\{\frac{1}{64}\right\} + 0.021$$

$$w = 0.027 \text{ psi}$$

The deflection can be found from the equation presented by Baumsister and Marks (1)

$$y = \frac{k_1 \, w \, r_1^4}{E} \frac{1}{T^3} \tag{10}$$

$k_1 = 0.14$

$r_1 = 1.166$ inch

$E = 5000$ psi

which gives

$$y = \frac{0.14 \times 0.027 \times 1.166^4}{5000} \times 64^3$$

$$y = 0.37 \text{ inch}$$

Although this deflection would require additional displacement of the diaphragm to balance the net effect of the volume change, it is not so extreme that failure would occur.

Based on the above calculations, a thickness of 1/64 inch was chosen for the neoprene as being adequate for an acceptable stress level. The resultant increase in the weight of the diaphragm system would be 0.43 pounds, which added to 8 pounds only gives a slight increase.

Appendix B. Overdesign Corrections

In the preliminary design of the initial plan, a mathematical error was found that exaggerated the requirements of the cam offset and the reservoir pressure. The correction is based on fundamental thermodynamics in that the cam offset allows the diaphragm to move through a displacement, causing a volume change, that is assumed to be an isentropic process of an ideal gas described by

$$PV^k = c \tag{11}$$

where k and c are constants. Differentiating this equation and dividing through by PV^k leads to

$$\frac{\partial P}{P} + k \frac{\partial V}{V} = 0 \tag{12}$$

which in terms of incremental changes would be

$$\frac{\Delta P}{P} + k \frac{\Delta V}{V} = 0 \tag{13}$$

Solving equation (13) for the change in volume, ΔV, and then substituting for the dimensions of the diaphragm that produces the change in volume gives

$$d\pi R^2 = - \frac{V}{k} \frac{\Delta P}{P} \tag{14}$$

where the negative sign indicates that a decrease in volume is required for the displacement to be positive. Solving equation (14) for the displacement gives the following corrected expression for the displacement:

$$d = - \frac{V}{\pi R^2 k} \frac{\Delta P}{P} \tag{15}$$

Theoretically the displacement for a 3.0 psf simulated sonic boom would then be 0.11 inch instead of the anticipated 0.97 inch.

The reservoir pressure was shown in the initial design to be dependent on the relationship in equation (15). Use of equation (15) would lead to a theoretical reservoir pressure of 10 psi for a 3.0 psf simulation rather than the 60 psi pressure that was originally expected.

Appendix C. Redesign of Drive System

In the process of locating the source of the nonlinear decay in the pressure signature, an investigation was made of the drive system to determine if belt slippage was occurring. A variable speed 3/4 hp D-C motor was driving the adjustable cam by two sets of V-belts and sheaves. The worse condition existed when the simulator was set for an 0.35 second duration, which gave a cam speed of 86 revolutions per minute. For sheave pitch diameters of 2.8 and 8.5 inches, the intermediate shaft speed would be

$$N_3 = \frac{D_4}{D_3} N_4 = \frac{8.5}{2.8} \times 86 = 261 \text{ rpm} \qquad (16)$$

By use of this speed and the diameter of 2.8 inches, the load carrying capacity of the second belt from the motor is given by the manufacturer (3) to be 0.46 horsepower. The problem was that when the single revolution clutch was activated, the impact loading on the belts required at least 1.25 horsepower. This was correctible by either increasing the diameter of the sheaves or by use of multiple belts. Both methods required replacement of the sheaves, so a combination of both was used. An increase in the diameter of the larger sheaves would add to the inertia of the system, but a 9.0 inch pitch diameter limit was imposed for clearance from the mounting table. The smaller sheaves diameter could then be determined by using the maximum motor speed of 1725 revolutions per minute and by taking a cam speed of 375 revolutions per minute.

The higher cam speed would give duration times as low as 0.08 second, which is more conformable to smaller aircraft. Using a consecutive numbered subscript for reference to the respective position of the sheaves from the motor, allows the speed and diameter relations to be given as

$$N_1 D_1 = N_2 D_2 \tag{17}$$

$$N_3 D_3 = N_4 D_4 \tag{18}$$

The second and third sheaves are attached to the intermediate shaft so their speeds would be identical, i.e., $N_2 = N_3$. Solving equations (17) and (18) for the speeds N_2 and N_3, and equating gives

$$\frac{N_1 D_1}{D_2} = \frac{N_4 D_4}{D_3} \tag{19}$$

For equal speed reductions of the two sets of sheaves, the same diameters must be used in each set, or

$$D_1 = D_3 \tag{20}$$

$$D_2 = D_4 \tag{21}$$

substituting (20) and (21) into (19) and solving for the first diameter gives

$$D_1 = \left\{ \frac{N_4}{N_1} D_2^2 \right\}^{\frac{1}{2}} \tag{22}$$

Therefore, using values previously given, the diameter of the smaller sheave is

$$D_1 = \left\{ \frac{375}{1725} \times 9.0^2 \right\}^{\frac{1}{2}}$$

$$D_1 = 4.2 \text{ inches}$$

To determine the load carrying capacity of the system, the intermediate shaft speed for the new diameter sheaves is needed

$$N_3 = \frac{D_4}{D_3} N_4 = \frac{9.0}{4.2} \times 86 = 184 \text{ rpm} \qquad (23)$$

The rating of the system based on double belts would be 1.58 horsepower, as given by the manufacturer (3). Thus the system would be capable of delivering power under the severe loading conditions that exist. A brief description, followed by the manufacturer's part number of the replacement parts, are listed below:

a. Browning gripnotch belt, AX46

b. Browning FHP sheave, 2AK46H

c. Browning FHP sheave, 2AK94H.

Appendix D. List of Symbols

a = acceleration

A = area of diaphragm

c = constant

d = displacement of diaphragm, i.e., cam offset

D = duration

dB = decibels

D_i = diameter of sheave (i = 1, 2, 3, 4)

E = modulus of elasticity

F = force

g = gravity constant

k = constant

k_1 = constant

m = mass

msec = milliseconds

N_i = angular speed of sheave (i = 1, 2, 3, 4)

oct = octave

P = pressure

psf = pounds per square foot

psi = pounds per square inch

$|P(w)|^2$ = energy spectral density

r = radius of lightening holes in diaphragm

r_1 = distance between diaphragm and control volume outer wall

R = radius of diaphragm

rpm = revolutions per minute

S = stress

t = rise time

T = thickness of neoprene

V = volume

w = total distributed load

w_a = inertial distributed load

w_o = distributed load from overpressure

y = deflection of neoprene at clearance space

Δ = incremental difference

Δf = bandwidth

ΔP = overpressure

ρ = density

π = constant

∂ = partial derivative designation